Observations with SPECT on the Normal Regional Distribution of Pulmonary Blood Flow in Gravity Independent Planes

Robert Lisbona, Geoffrey W. Dean, and Tawfic S. Hakim

Nuclear Medicine Department, Royal Victoria Hospital; and Department of Physiology, McGill University, Quebec, Canada

While the effect of gravity on the pulmonary circulation is well documented, the distribution of pulmonary flow under gravity independent conditions is not as well understood. Single photon emission computed tomography was applied to the study of regional pulmonary blood flow in slices where the effect of gravity was constant. Lung tomography, after the injection of [^{99m}Tc]MAA, was carried out in six normal volunteers and in the fully inflated and isolated lungs from six dogs that had been killed. Our tomographic results suggest that pulmonary perfusion in isogravitational planes is inherently nonuniform with preferential flow centrally and reduced circulation more peripherally. Planar imaging of the dissected isogravitational slices from the animals further confirmed the uneven perfusion noted on the tomographic slices.

J Nucl Med 28:1758–1762, 1987

It is well established that, in the normal erect subject, the distribution of blood flow to the lung from the pulmonary artery is strikingly nonuniform (*1,2*). Much emphasis has been placed on the role of gravity that greatly influences regional resistance through its effect on the caliber of the capillaries (*3*). Arterial, venous, and alveolar pressure differences are basic elements that regulate blood flow through the lungs and the impact of gravity in inducing a zonal stratification of perfusion (zone 1–4) has been thoroughly documented (*4*). The purpose of this communication is to evaluate, using single photon emission computed tomography (SPECT), the normal distribution of lung blood flow under conditions that minimize the effect of gravity.

MATERIALS AND METHODS

Studies in the Human

The subject population consisted of six normal male volunteers, aged 20–36 yr, with no evidence of lung disease or history of cigarette smoking. The volunteers were injected while supine with 5 mCi (185 MBq) of technetium-99m macroaggregates of albumin ([^{99m}Tc]MAA) after resting in that recumbent position for 5 min. The radiopharmaceutical was administered through an antecubital vein during a 15-sec breathold with open glottis and at normal end expiration (FRC). The approximate number of particles injected was 500,000, more than 90% of which ranged between 10–70 microns in diameter. SPECT imaging was then undertaken after positioning the thorax within the field of view of an integrated tomographic system* equipped with a low-energy, high resolution collimator. One hundred and twenty projections of the lungs were registered from a circular orbit in 128×128 matrices and in 3-degree steps around the subject. Each projection was generated over 10 sec and accumulated some 100,000 counts. The subjects held their breath during the imaging interval but breathed during the 2 sec required by the camera head to rotate to its next projection angle. The data were then reconstructed by filtered backprojection using a third order Butterworth filter with a cutoff frequency of 0.3 times the Nyquist frequency which, in the system discussed herein, was 0.127 cm^{-1}. There was no attenuation correction. Tomographic sections 11-mm thick were reconstructed in the transverse, sagittal, and coronal planes. In order to remove remaining reconstruction artifacts from each slice, pixels with a value of < 10% of the maximal activity of that slice were set to zero. Thereafter, count rate profiles and mappings of the distribution of radioactivity were created from the coronal slices whereby each slice represented an isogravity plane since all its elements were at the same horizontal level both at the time of injection of the radiotracer and also at the time of imaging.

Animal Studies

Six healthy large mongrel dogs (mean weight of 30.5 kg) were anesthetized with 25 mg/kg of sodium pentobarbitol.

Received Nov. 25, 1986; revision accepted May 11, 1987.

For reprints contact: Robert Lisbona, MD, Dept. of Nuclear Medicine, Royal Victoria Hospital, 687 Pine Ave. West, Montreal, Quebec H3A 1A1 Canada.

The intubated animals were placed supine and were hemodynamically monitored with Swan-Ganz Catheterization. When the animals were stabilized and breathed spontaneously, 20 mCi of [^{99m}Tc]macroaggregated albumin (15–70 microns in diameter) were injected, at end expiration over several breaths, through the proximal port of the Swan-Ganz Catheter into the superior vena cava. The embolized particles caused no detectable hemodynamic effect. Thereafter, the animals were killed by rapid exsanguination, the chest opened, and the heart and lungs removed en bloc. The lungs were separated from the mediastinal structures and passively drained of their remaining blood content. They were then inflated to total capacity by blowing air into them at a temperature of 50°C and a constant pressure of 35 cm H_2O. The surface of adjacent lobes were subsequently glued to maintain the inflated lobes in fixed position, as they would be in the thoracic cavity. The air drying process of the lungs continued for 18–20 hr. At the end of that time period, the extracted canine lungs were imaged tomographically, as in the human, to evaluate the distribution of radioactivity in the isogravity coronal planes. Each projection image, however, was generated over an interval of 15 sec. Furthermore, mid-coronal (10 mm thick) slabs of lung tissue were dissected out from the dry lung preparations and imaged in planar fashion directly by placement on the surface of the appropriately collimated camera head. Imaging time was 6 min and yielded on the average 260,000 counts.

RESULTS

Human Studies

A mapping of the distribution of radioactivity at mid-coronal level was plotted from the reconstructed data for each of the volunteers. This mapping was characterized by a marked nonuniformity in the distribution of radioactivity, and hence perfusion, with a maximal concentration of counts deep within the slice relative to the periphery (Fig. 1). The mappings repeatedly revealed that perfusion was unequal even though the force of gravity was constant throughout the mid-coronal plane. Because of the uniform thickness of the reconstructed slices and the similar air volume in the alveoli, which would be equally inflated at the same horizontal level, the tomographic image of the slice suggests therefore that blood flow per unit volume of the lung in an isogravitational plane is markedly uneven and is highest centrally. The central regions were up to ten times more perfused than the periphery depending on the definition of the edge. Coronal slices from all levels also revealed a similar pattern of inequality. This is illustrated in Figure 2 where count rate profiles generated from anterior, posterior, and mid-coronal slices are shown. The curves consistently showed a clustering of activity deep within the lung slice with a gradual tapering of the counts outwardly from the maximum. As this pattern of nonuniformity was noted from the most anterior plane to the most posterior one, with peak counts in the mid-coronal slice, the indication then is that on a three dimensional level there is preferential perfusion to the core of the lung relative to its periphery.

Animal Studies

There were many technical advantages to the animal experiments. The excised lungs gave us the opportunity to evaluate regional circulation under conditions which avoided the effect of attenuation and scatter from the chest wall, diaphragm, and mediastinal structures. A shorter radius about the axis of rotation could also be used during the acquisition period as the camera face was in much closer proximity to the organ of interest than was the case with the human volunteers. As well, the static specimens eliminated any disturbance from possible respiratory motion. Again, analysis of the tomographic data from the lung preparations revealed results similar to that of the humans. A marked central to peripheral gradient in blood flow was present in the canine lung, independent of gravity. Moreover, with isolation of the lungs, it was further documented that there is preferential perfusion to the center of each lobe

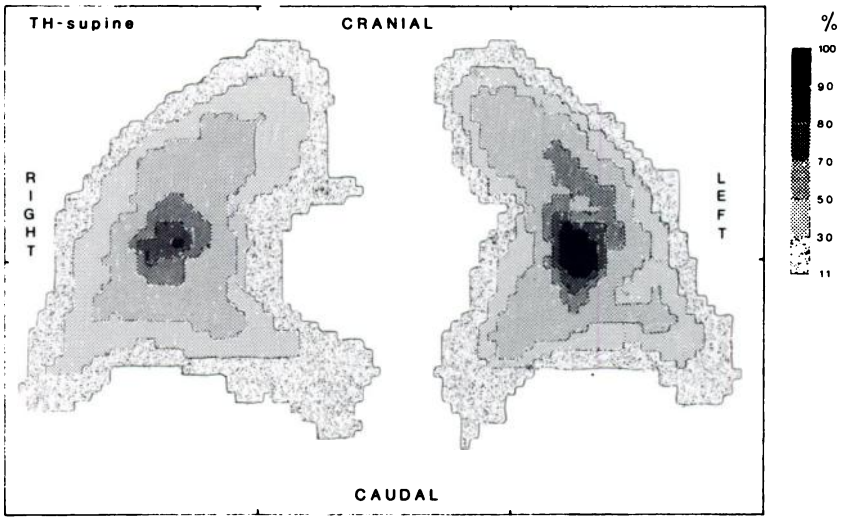

FIGURE 1
The mapping of the distribution of [^{99m}Tc]MAA in a representative mid-coronal and gravity independent section from a healthy individual reveals a marked uneveness of perfusion. Flow is maximal centrally, as denoted by the darkest areas of shading, and drops off gradually towards the periphery. The central to peripheral gradient of perfusion is ~10:1.

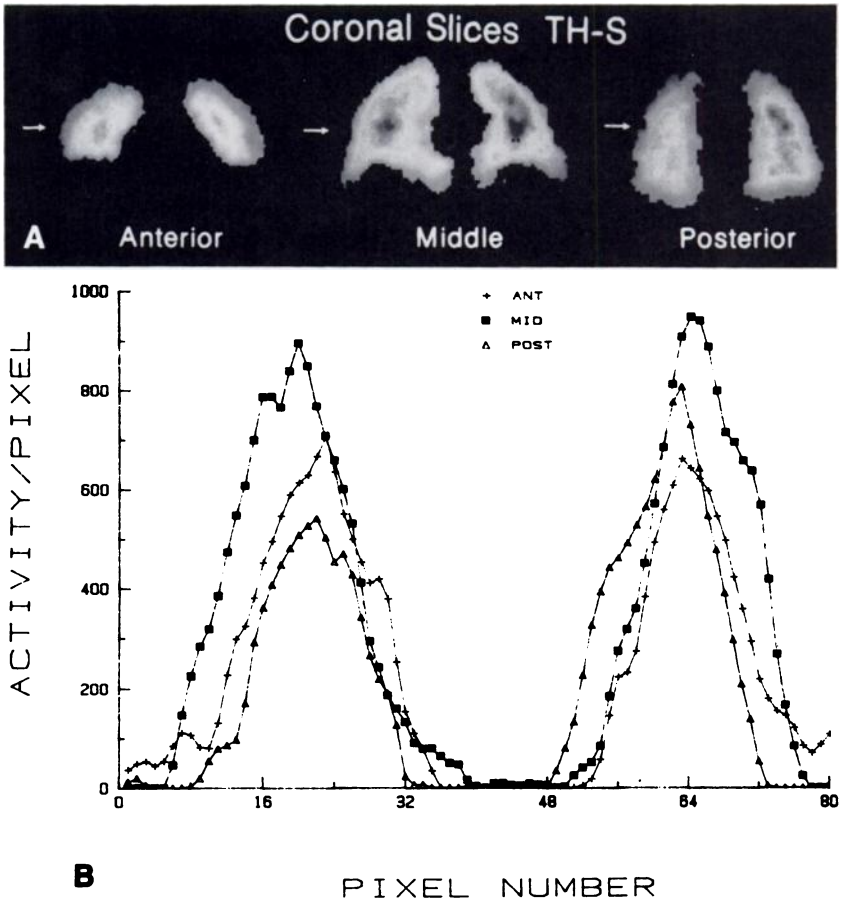

FIGURE 2
Three representative coronal slices from one subject and obtained at anterior, posterior, and mid-coronal levels also show peak activity centrally. B: Horizontal profiles of activity generated from the slices illustrated in Figure 2A, and at the level of the arrows, again reveal a central to peripheral gradient of perfusion. Peak activity is observed in the center of each section with maximal perfusion localized to the core of the mid-coronal slice.

relative to its periphery, although the center of the lower lobe was usually the site of maximal perfusion of the slice (Fig. 3).

Planar Imaging of 10-mm-Thick Coronal Slab

Quantitative analysis of the planar acquisition data from the mid-coronal slabs confirmed the results of the tomographic analysis. Namely that there was a dramatic inequality of pulmonary perfusion on the mapping of radioactivity which was independent of the effect of gravity. Pulmonary blood flow peaks centrally in the individual lobes and subsequently drops off in circumferential fashion to reach a minimal value in the peripheral rinds of parenchyma. In that phase of the study, the enhanced central perfusion of the individual lobes could also be appreciated.

DISCUSSION

Basic pulmonary physiology has always emphasized the importance of gravity in determining the distribution of pulmonary blood flow. Gravity can cause important inequalities in regional perfusion due to a gradual increase in the hydrostatic pressure down the pulmonary circulatory system (*3,5*). Classically, in the normal upright individual, pulmonary blood flow is minimal in the apices where P_{alv} exceeds P_a and P_v (zone 1). More caudally, in zone 2, P_a exceeds P_{alv} and flow is dictated by the differences between these pressures. In zone 3, when P_v finally exceeds P_{alv}, the latter becomes inconsequential and blood flow continues to augment in function of P_a and P_v differences. Basally, in zone 4, flow diminishes as interstitial pressures around the vessels increase.

While the theoretical effect of gravity on the pulmonary circulation is clear, the distribution of regional pulmonary flow in gravity independent conditions is more conflictual. Conventionally, it is thought that minimal irregularity in flow exists at isogravity levels. Newhouse et al. (*6*), using planar imaging and radioxenon, suggested that no significant perfusion gradient existed in man in the horizontal direction. This was supported by West et al. who concluded that flow became almost but not entirely homogeneous in isolated lungs with zero gravity simulated conditions (*7*). In contrast, more recently, Amos (*8*) reported that there is indeed inequality of flow at isogravity levels. There is also a growing body of experimental evidence suggesting that apart from the effect of gravity, there can be a marked nonhomogeneity of pulmonary blood flow. Greenleaf et al. (*9*) documented medial-lateral and apical-basal inequalities of flow at isogravity levels using

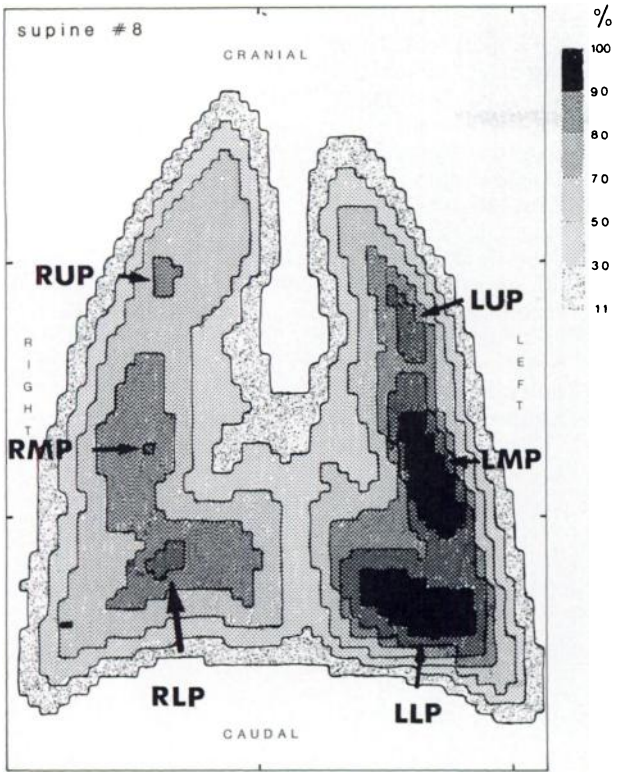

FIGURE 3
The mapping of the distribution of radioactivity at the mid-coronal level, from the reconstructed tomographic data of the isolated dry and fully inflated canine lung, shows non uniform perfusion. The most darkly shaded areas represent peak flow which is some ten times that noted in the periphery. Moreover, the pattern of preferential central perfusion seems to be duplicated at the level of the individual lobes: LLP = left lower lobe peak; LMP = left middle lobe peak; LUP = left upper lobe peak; RLP = right lower lobe peak; RMP = right middle lobe peak; RUP = right upper lobe peak.

labeled microspheres. Others have also noted, in the canine lung, a central to peripheral distribution of blood which is independent of the effect of gravity (*10*). In an intricate and demanding experiment, with dissection of postmortem dry lungs and analysis of individual samples throughout slices of the organ, it was found that the core of isogravity sections was preferentially perfused (*11*).

SPECT imaging is a relatively simple method that allows for the noninvasive and quantitative study of the three dimensional distribution of the pulmonary circulation (*12–14*). With the technology of SPECT, uniform thickness slices and equal volumes of lung tissue could be selected along isogravitational planes to assess blood flow both in the human and in the excised animal lung. Our observations suggest that lung perfusion in the normal subject at rest is inherently nonuniform, independent of gravity which, of course, can still further influence whatever regional differences exist. These findings therefore represent a fundamental shift in emphasis as to factors dictating regional pulmonary blood flow. They also provide a greater understanding of zone 4 which appears to be the two dimensional manifestation of a three dimensional phenomenon.

Anatomic features such as major vessels and airways can interfere with the measurement of regional flow by simply reducing the relative amount of lung parenchyma per unit volume of the organ (*14*). It is unlikely, however, that our findings are only artifactual and due to partial volume effects since they were noted throughout the lung and at many sites where large airways and vascular channels should be of no hindrance. Instead, the preferential perfusion which we noted to the core tissue of the lung, or even of a lobe, could well reflect the varying resistance of the delivery circuits. Conceivably, in the lung periphery, there is increased resistance in flow induced by the long delivery pathways of the vessels which, originating from the central main arteries, perfuse the distant lung. This resistance can reduce the outward magnitude of flow and help confine perfusion to the shorter and lower resistance channels bathing the inner lung. In states requiring high pulmonary blood flow rates, (e.g., exercise where cardiac output can increase fivefold) recruitment of vasculature can then occur from the center of the organ outwards. The potential for increasing flow seems to exist therefore in all directions rather than along a vertical axis only (*3*), further highlighting the capacity of the pulmonary vascular system to recruit more vascular channels. These hypotheses and the distribution of pulmonary blood flow in disease states are currently being investigated in our department with SPECT. Tomography should also contribute to the three dimensional understanding of the distribution of ventilation which should match that of perfusion to maximize gas exchange (*15,16*).

NOTE

*(Technicare Omega 500-MCS 560) Technicare, Solon, OH.

REFERENCES

1. Anthonisen NR, Milic-Emili J. Distribution of pulmonary perfusion in erect man. *J Appl Physiol* 1966; 21:760–766.
2. Hughes JMB, Glazier JB, Maloney JE, et al. Effect of lung volume on the distribution of pulmonary blood flow in man. *Respir Physiol* 1968; 4:58–72.
3. West JB, Dollery CT, Naimark A. Distribution of blood flow in isolated lungs relation to vascular and alveolar pressures. *J Appl Physiol* 1964; 19:713–724.
4. Hughes JMB, Glazier JB, Maloney JE, et al. Effect of extra-alveolar vessels on distribution of blood flow in the dog lung. *J Appl Physiol* 1968; 25:701–712.
5. Permutt S, Bromberger-Barnea B, Bane HN. Alveolar pressure, pulmonary venous pressure and vascular waterfall. *Med Thorac* 1962; 19:239–260.
6. Newhouse MT, Wright FJ, Ingham GK, et al. Use of

scintillation camera and Xenon-135 for study of topographic pulmonary function. *Respir Physiol* 1968; 4:141–153.
7. West JB, Dollery CT, Matthews CME, et al. Distribution of blood flow and ventilation in saline-filled lung. *J Appl Physiol* 1965; 20:1107–1117.
8. Amis TC, Jones HA, Hughes JMB. Effect of posture on inter-regional distribution of pulmonary perfusion and V/Q ratios in man. *Respir Physiol* 1984; 56:169–182.
9. Greenleaf JF, Ritman EL, Sass DJ, et al. Spatial distribution of pulmonary blood flow in dog in left decubitus position. *Am J Physiol* 1974; 227:230–244.
10. Beck KC, Rehder K. Differences in regional vascular conductances in isolated dog lungs. *J Appl Physiol* 1986; 61:530–538.
11. Hakim TS, Lisbona R, Dean GW. Gravity non-dependent distribution of pulmonary blood flow. In: Will JA, Buckner CK, Dawson CA, et al., eds. The pulmonary circulation in health and disease. New York: Academic Press, 1986: in press.
12. Macey DJ Marshall R. The lung. In: Ell PJ, Holman BL, eds. Computed emission tomography. New York: Oxford University Press, 1982: 495–520.
13. Maeda H, Itoh H, Ishii Y, et al. Pulmonary blood flow distribution measured by radionuclide-computed tomography. *J Appl Physiol* 1983; 54:225–233.
14. Osborne D, Jaszczak RJ, Greer K, et al. SPECT quantification of Technetium-99m microspheres within the canine lung. *J Comp Assist Tomogr* 1985; 9:73–77.
15. Lavender JP, Al-Nahhas AM, Myers MJ. Ventilation perfusion ratios of the normal supine lung using emission tomography. *Br J Radiol* 1984; 57:141–146.
16. Klumper A, Zwijnenburg A. Dual isotope ($^{81}Kr^{m}$ and $^{99m}Tc^{m}$) SPECT in lung function diagnosis. *Phys Med Biol* 1986; 31:751–761.